STUDY OF FREE FALLING LIQUID LAYER IN INCLINED PIPES: EFFECT OF DIAMETER AND INCLINATION ANGLE

J. S. Lioumbas[1], O. J. Nydal[2], S.V. Paras[1]

[1]Department of Chemical Engineering, Aristotle University of Thessaloniki
Univ. Box 455, GR54124 Thessaloniki, Greece.

[2]Department of Energy and Process Technology, NTNU
N-7491, Trondheim, Norway.

ABSTRACT

The work reported here is part of a study concerning gas-liquid co-current downflow in inclined pipes. Since the understanding of free flowing liquid layer characteristics is considered a first step towards interpreting the co-current gas/liquid flow mechanisms, it is believed that an accurate characterization of waves developed in the absence of gas flow will improve our physical understanding of the more complicated stratified two-phase flow.

With the intention to study the effect of tube diameter and inclination angle on the mechanisms triggering wave formation on the liquid interface, experiments were conducted with tap water at atmospheric pressure, in pipes with various diameters (i.e. 24, 32 and 60mm) and inclination angles with respect to the horizontal position (1-9deg). For almost all pipe diameters and inclination angles tested, visual observations and layer thickness time records reveal the existence of four distinct regions on the basis of the wave patterns observed and the evolution of solitary waves at relatively low Reynolds numbers. Impedance probes (i.e. parallel wires and ring probes) were applied for layer thickness measurements. The values of mean layer thickness, *RMS* and power spectra of the fluctuations, as well as wave celerity, were calculated. A simplified model based on a modified force balance is proposed for the prediction of the mean layer thickness and found to be in good agreement with the experimental data.

1. INTRODUCTION

The stratified flow regime is frequently encountered in long distance transfer pipelines (e.g. oil flows and natural gas) and in power generation, petrochemical and process plants. The work reported here is part of a study concerning stratified gas liquid co-current downflow in inclined pipes, where the gravity-induced wavy liquid layer plays a dominant role. Understanding the free flowing liquid layer characteristics is considered a first step before introducing the complication of co-current gas/liquid flow.

Mass and heat transport across gas liquid interface is very important for the chemical industry (e.g. chemical reactors, boilers, steam condensers, heat exchangers and gas absorbers), because interfacial waves enhance both heat and mass transfer. Moreover, falling liquid layers are commonly used due to their relatively high energy and mass transfer potential at low liquid flow rate [1]. Extensive research work, both experimental and theoretical, carried out over the last few decades suggests that the rate of momentum, heat and mass transfer is strongly influenced by the layer characteristics and especially by the waviness of the gas-liquid interface.

Despite over fifty years of research, a generally accepted mechanism explaining the role of the interfacial waves in the transport of heat, mass or momentum across the gas-liquid interface is not available mainly due to the complexity of the flow [1]. It is, therefore, considered advantageous to use relevant information on wavy free falling liquid layers in order to enhance our physical understanding of the more complicated case of co-current gas-liquid flow in inclined pipes for a range of relatively low Reynolds numbers (200~2000). Regardless of the progress made in recent years, significant gaps exist in understanding and modeling the evolution of free flowing liquid layers. To contribute in this direction, the present work aims at obtaining complete sets of detailed data on layer flow inside slightly inclined pipes.

Free flowing liquid layers were first studied by the fatherson team of the Kapitza family [2], who conducted simple experiments on an inclined plane at a Reynolds number of about 100. This pioneer work was followed by a plethora of studies regarding liquid layer flow on inclined or vertical planes [3, 4, 5, 6, 7]; however, and to the authors' best knowledge, systematically obtained data on free falling layer thickness for various pipe diameters and inclination angles in a range of low to moderate Reynolds number are not available in the literature. Wilkes and Nedderman [8], who worked with glycerine solutions in a 3m vertical tube (25mm i.d), provided the first measurements of the velocity profiles under thin wavy layers and concluded that the velocity profile under a wavy layer remains parabolic, i.e. similar to Nusselt flat layer. Stainthorp and Allen [9] performed a set of experiments for very low Reynolds numbers (4-45), using water inside a 76cm long vertical glass tube (i.d.=3.45cm) and reported that, for naturally excited waves, the wave profile, wavelength and wave celerity change significantly downstream the wave inception. Giovinne et al. [10] investigated the stability of liquid flow down an inclined pipe using linear stability analysis and concluded that after a certain value of the liquid height the flow retains its stability. Quite recently Mouza et al. [11], who studied the influence of small tube diameter on falling layer and flooding

suggest that the tube curvature strongly affects the liquid layer flow development, possibly promoting wave interaction and damping.

The main objective of the work reported here is to obtain accurate measurements of layer thickness variation with time over a wide range of liquid Reynolds numbers, pipe diameters and inclination angles. It is believed that these new data will improve our physical understanding of free flowing thin liquid layers.

In this paper a description of experimental equipment and procedures is presented first. Experimental data on free falling layers are reported and various statistical quantities are extracted from layer thickness time records (e.g. layer height, statistical characteristics) that facilitate the interpretation of liquid layer behavior.

2. EXPERIMENTAL SET-UP AND PROCEDURES

To study the effect of the pipe diameter, three test sections having a diameter of 24, 32 and 60mm respectively were used. Experiments were conducted at ambient temperature and pressure conditions at two different rigs, using tap water.

- The *first* rig, located at the Laboratory of Chemical Process and Plant Design at Aristotle University of Thessaloniki (*A.U.Th.*), is a 24mm i.d. Plexiglas® tube with a 7m long straight section, which can be rotated up to 15deg from the horizontal to enable downward flow. Filtered tap water is stored in a 70 l tank and recirculated by means of a centrifugal pump.
- The *second* rig, located at the Multiphase flow laboratory at Norwegian University of Science and Technology (*NTNU*), comprises of two straight pipes each 16.5m long made of transparent acrylic PVC and having 32mm and 60mm i.d., respectively. The flow rig can be rotated up to 15deg from the horizontal. The water, before entering the loop, is directed through an overflow that diminishes the pressure differentiations triggered by pump oscillations.

The liquid flow rate is measured using a bank of calibrated rotameters in the first rig, while in the second rig a bank of electromagnetic flow meters was applied in order to cover the range of the present experiments; the accuracy of the flow meters is better than $\pm 1\%$. For liquid layer thickness and wave celerity measurement, parallel wire conductance probes on the symmetry plane were used in the *first* flow loop while in the *second* loop conductance ring probes were applied. The techniques used in both cases are based on the inverse proportionality between electrical resistance of the liquid layer and its thickness. Details of the measuring techniques can be found elsewhere [12], [13]. The liquid Reynolds number, Re_L:

$$\mathrm{Re}_L = \frac{U_{LS} D}{\nu} \tag{1}$$

is based on the superficial liquid velocity, U_{LS}, defined as:

$$U_{LS} = \frac{Q_L}{A} \tag{2}$$

To compensate for temperature effects the liquid conductivity was measured both prior to and after of each set of experiments and a correction factor was incorporated in the layer thickness calculation. The accuracy of the measurements throughout the set of the experiments is estimated to be around $\pm 10\%$ taking into account uncertainties in the calibration procedure (e.g. temperature variations). The statistical quantities and other parameters of the layer thickness time records (i.e. *RMS* and spectra of the fluctuations, mean wave height, wavelength, and wave celerity) were calculated from 12,000-point samples, obtained over a period of 60s with a 200Hz sampling frequency.

3. EXPERIMENTAL RESULTS

3.1 Visual observations

In this section an overview of the falling liquid layer interfacial structure is provided, obtained by visual observations of the flow in pipes with diameters 24, 32 and 60mm. Four distinct flow regions can be readily identified (***Figure 1***):

- For the smallest Reynolds numbers employed, small amplitude waves (ripples) are observed on the liquid surface (*Region I*). Patnaik and Blanco [14] have also described this kind of waves in detail even though their study refers to falling layers on inclined plates.
- As the liquid flow rate increases the liquid interface turns practically smooth and undisturbed (*Region II*). Park and Nosoko [15], although they examined the free falling water layer characteristics inside **vertical** pipes for Re_L~400, reported a similar behavior, i.e. transition from a wavy to an undisturbed interface with increasing flow rate.
- For even higher Re_L *solitary waves,* traveling along the pipe on the liquid interface, make their appearance at a distance of approx. ***30-50*** pipe diameters (depending on pipe diameter and inclination angle) from the liquid entrance (*Region III*). A *critical* Reynolds number, Re_{LC}, is related to the appearance of these solitary waves, which are relatively large amplitude coherent waves that are nearly two-dimensional and retain their original shape while traveling along the pipe. Visual observations reveal that a rather undisturbed flat layer separates them and their wavelength, which depends on pipe diameter and inclination, decreases as the diameter and inclination angle increases.
- As the flow rate further increases, the solitary waves become more frequent, retain their original amplitude and merge forming *3D* structures (*Region IV*).

The above behavior is noticeable for all pipe diameters (24mm, 32mm and 60mm) and inclination angles tested. It must also be noted that the transition between the regions is shifted to lower Re_L as the pipe diameter and inclination angle increases. Moreover, the extent of *Region III* is reduced as the inclination angle increases and tends to disappear for the larger pipe diameters (i.e. 60mm). For example, in the 24mm pipe the solitary waves are observed for ***all*** inclination angles examined; for the 32mm pipe the solitary waves make their appearance only at 1deg and 2deg inclination, whereas in the 60mm pipe they appear ***only*** at 1deg**.** Consequently, it could be assumed that the occurrence of primary liquid layer instabilities observed in *Region III* increases as the pipe diameter decreases.

3.2 Liquid layer characteristics

Using the experimental procedures described in a previous section, the free-flowing liquid layer thickness was measured:

- for an inclination range, β, of 1-9deg for the 24mm i.d.
- for an inclination range of 1-3deg for the 32mm and 60mm i.d.

for various flow rates covering a Re_L range from ~200 to ~2200 at a pipe location where the flow can be considered developed, i.e. in the 24mm i.d. pipe measurements were performed 6m downstream the inlet, whereas in the 32mm and 60mm i.d. pipes measurements were made 7m and 8m from the inlet, respectively.

Typical liquid layer traces for the 24mm pipe at 1deg inclination angle are presented in ***Figure 1***, where the regions described in the previous section are readily observed. That is, for Re_L=180 (***Figure 1a***) the trace corresponds to *Region I*, where small amplitude waves appear on the liquid surface. As the liquid flow rate increases (***Figure 1b***) the liquid interface turns practically smooth and undisturbed (*Region II*). When Re_L=750 is reached (***Figure 1c***) high amplitude solitary waves are the dominant features (*Region III*). A further flow rate increase (Re_L =1240) results to a flow pattern that corresponds to *Region IV* (***Figure 1d***), where high-frequency small-amplitude waves can be easily observed.

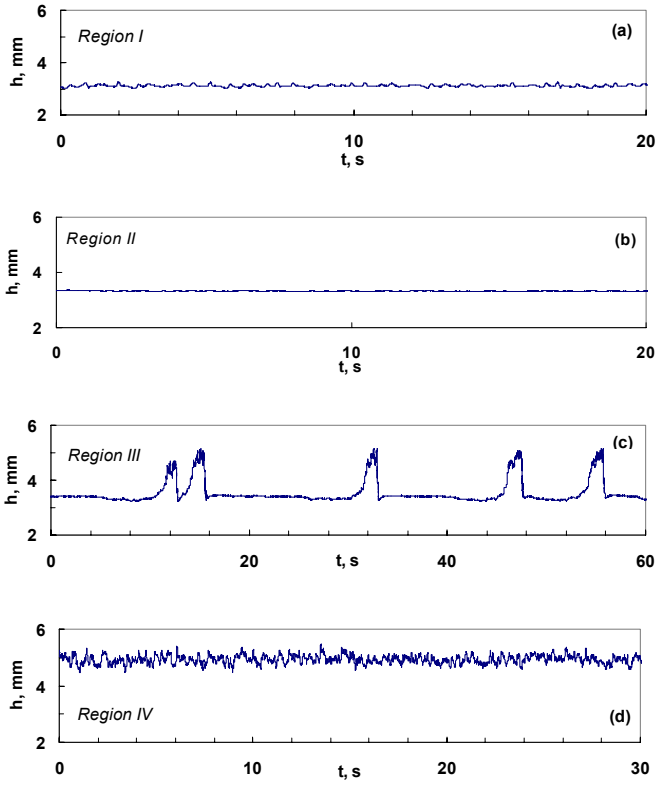

Figure 1. Typical layer thickness traces for D = 24mm and β = 1deg (a) Re_L=180; (b) Re_L=450; (c) Re_L=750; (d) Re_L=1240.

The time series of the layer thickness data are statistically analyzed to obtain the main layer characteristics, namely the mean thickness, h_{mean}, the root mean square of the thickness, h_{rms}, the maximum wave height, h_w, and the undisturbed liquid layer thickness, h_s, as well as the mean wave height above the undisturbed liquid layer, $\Delta h = h_w - h_s$ (***Figure 2***).

The calculated h_{mean} results, presented in ***Figures 3 & 4,*** show that h_{mean}:

- decreases as the inclination angle increases and
- has a tendency to increase with the pipe diameter; this trend seems to be clear for Re_L > 500 (*Region II-III & IV*).

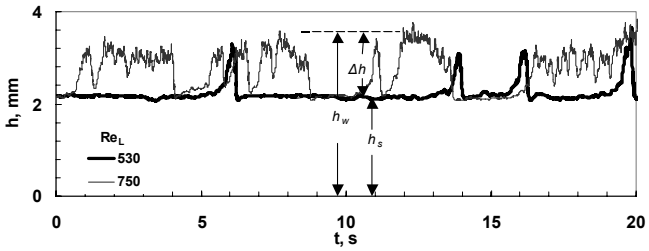

Figure 2. Typical layer thickness traces in Region III for D=24mm and β=4deg.

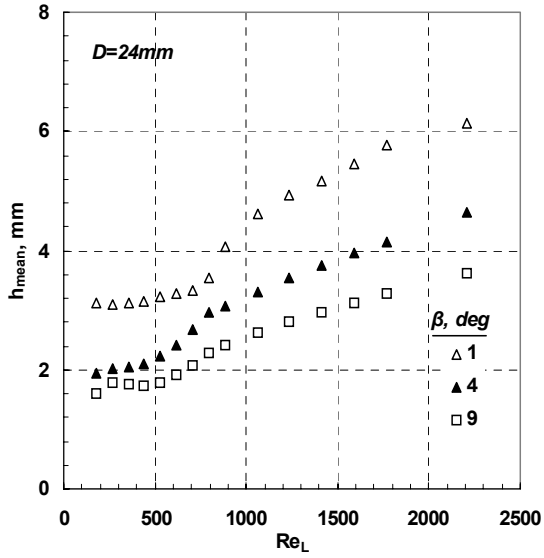

Figure 3. Mean layer thickness vs Reynolds number; inclination effect for D=24mm.

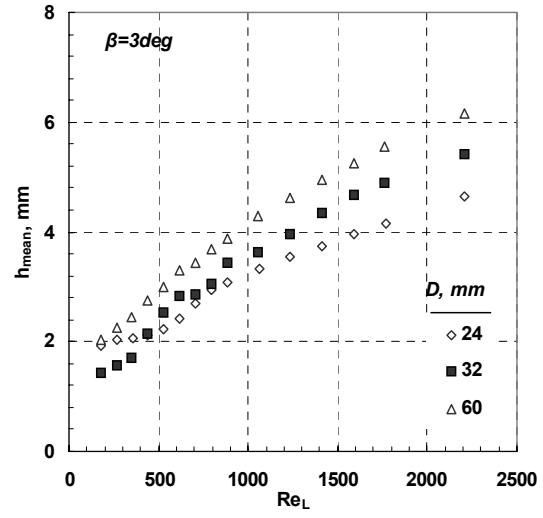

Figure 4. Mean layer thickness vs Reynolds number; pipe diameter effect for β=3deg.

In ***Figure 5a & 5b*** the dependence of h_{rms} on Re_L for the 24mm i.d and 60mm i.d. pipe respectively and for various inclinations is presented.

The power spectral density *(PSD)* of the layer thickness time series have been obtained by averaging modified periodograms [12]. The error in the computed spectra is 12% and their resolution is approximate 0.2Hz. Typical *PSD* of the layer thickness fluctuations at various Re_L corresponding to *Regions I, III and IV* are presented in ***Figure 6*** for the 24mm i.d. pipe and β=4deg. The modal frequency, f_m, increases with the flow rate in *Regions III* and *IV*, a fact that is consistent

with the visual observations. In addition, the area under the curves is related with the amplitude of the waves observed in the corresponding regions (***Figure 1***). The modal frequency, f_m, calculated for all wave traces, is plotted versus the corresponding Re_L and it is found to increase with the pipe diameter and inclination angle (***Figures 7a*** & ***7b***).

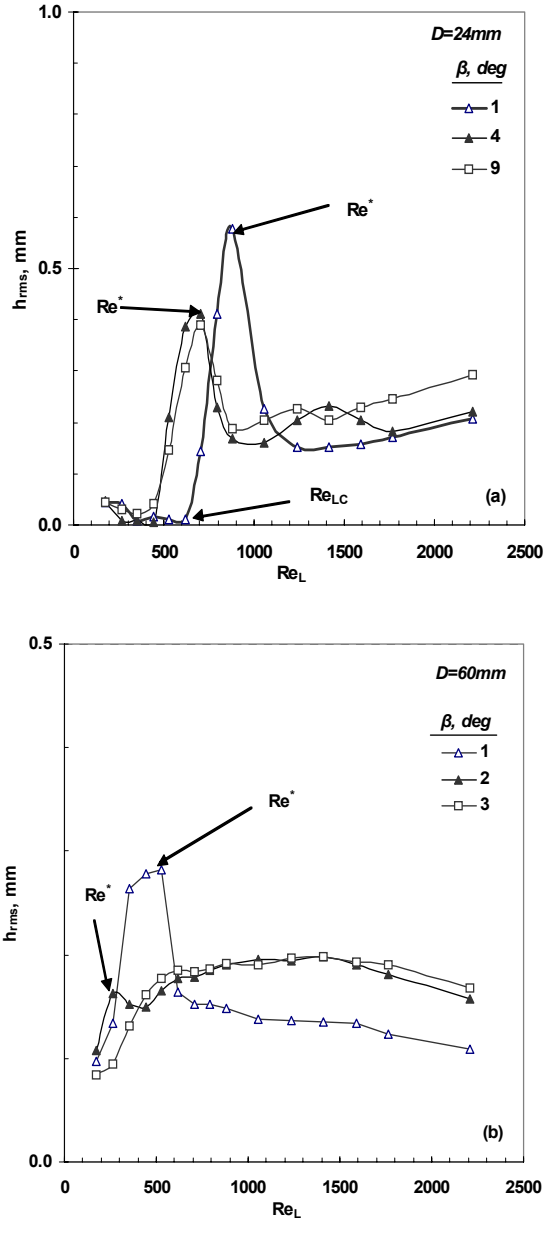

Figure 5. Effect of pipe inclination on h_{rms} values: a) D=24mm; b) D=60mm.

The celerity, c, of the waves is calculated by cross-correlating two layer thickness signals recorded simultaneously at two neighboring locations, (i.e. 30mm, 80mm and 160mm apart for the 24mm 32mm and the 60mm i.d. pipe respectively). The results are presented in ***Figures 8a*** & ***8b***, where the wave celerity is drawn against Re_L for various pipe inclination angles and diameters, respectively. The wave celerity increases with inclination angle, an effect that is more pronounced at the higher Re_L employed. The pipe diameter affects the wave celerity but not in a proportional way, that is at a certain Re_L value the celerity increase between the 24 and 32mm pipe is much larger than the one observed between the 32 and 60mm pipe.

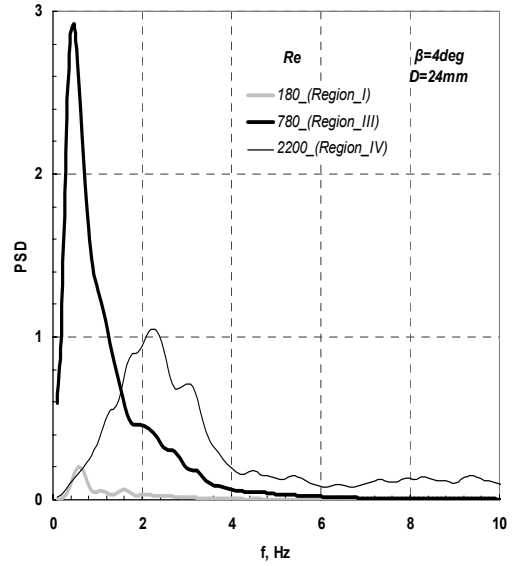

Figure 6. PSD of liquid layer thickness, D=24mm, β=4deg.

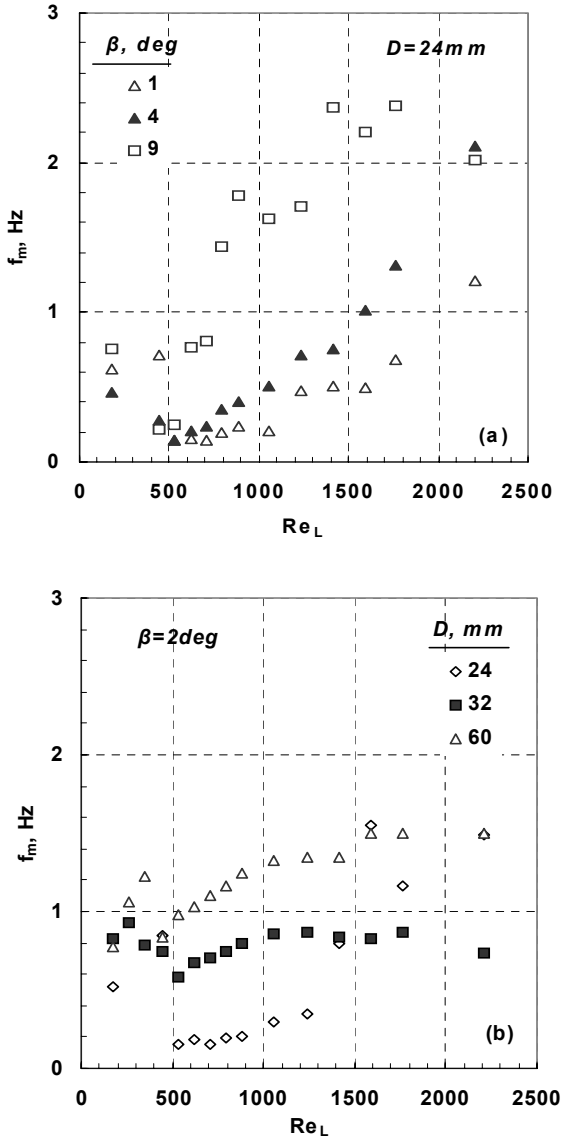

Figure 7. Modal frequency dependence on Re_L for: (a) various inclinations; (b) various pipe diameters.

In ***Figure 9***, both the wave celerity and the Δh values for the same geometry (24mm i.d pipe for 1deg inclination) are presented.

The various regions, identified by visual observations in a previous chapter, can be distinguished as follows:

- ***Region I***: In this region, where the first small ripples are observed, the Δh values and the wave celerity are relatively low.
- ***Region II***: As the flow rate increases Δh values **become** even smaller than those observed in *Region I*, since the ripples tend to diminish and the liquid interface becomes practically smooth. Consequently, no celerity data is reported for this region. It must be noted that as pipe diameter and inclination increases this region tends to disappear.
- ***Region III***: This region begins at $\boldsymbol{Re_{LC}}$ and corresponds to a sudden increase of the Δh values, a behavior attributed to the presence of solitary waves (***Figure 1c***). When the flow rate increases further the solitary waves become more frequent and a maximum value, Δh_{max}, is reached at a Reynolds number $\boldsymbol{Re^*}$. It is interesting to notice that, although the flow rate increases, the mean wave height, Δh, and the undisturbed liquid layer, h_s both remain practically constant as shown in ***Figure 2***. It must also be noted that, as pipe diameter and inclination angle increases, Re^* is shifted to lower values, while the h_{rms} value decreases (***Figure 5***).
- ***Region IV***: A further Re_L increase leads to a strong reduction of the Δh value, **a fact** attributed to the presence of more frequent solitary waves, which tend to merge resulting in higher h_{mean} (***Figure 3***) and a smaller h_{rms} (***Figure 5a***). For even higher flow rates, Δh values tend to become practically independent of Re_L. In this region the h_{rms} increases with pipe inclination (***Figure 5***), since the gravity component perpendicular to the flow direction (which exerts a stabilizing effect) is getting smaller.

The wave celerity minimum at *Region III* corresponds to the maximum Δh value observed. Stainthorp and Allen [9] reported a similar behavior for the wave celerity, although their experiments refer to wavy liquid flow *outside* a vertical cylinder. This tendency is observed for **all** inclination angles and pipe diameters employed and it is attributed to the appearance of solitary waves at this particular Re_L region. This behavior is consistent with the fact that, in order to comply with the mass conservation principle, an increase of the solitary wave frequency must be accompanied by a relevant decrease of their celerity.

4. INTERPRETATION OF LAYER THICKNESS DATA

The approach proposed by Mouza et al. [16] valid for a laminar free-falling layer in a cylindrical tube, is employed here to compute the mean thickness, h_{mean}, using as basic input quantities the liquid flow rate, tube i.d., tube inclination angle, β, and fluid physical properties. As shown in ***Figure 10a*** there is a fairly good agreement between measured values and the predictions from the above model **only** for a Reynolds number region Re_L<750. It is obvious (***Figure 10b***) that, for the larger pipe diameters, where *Regions I* and *II* tend to disappear, the laminar model does not agree with the experimental data.

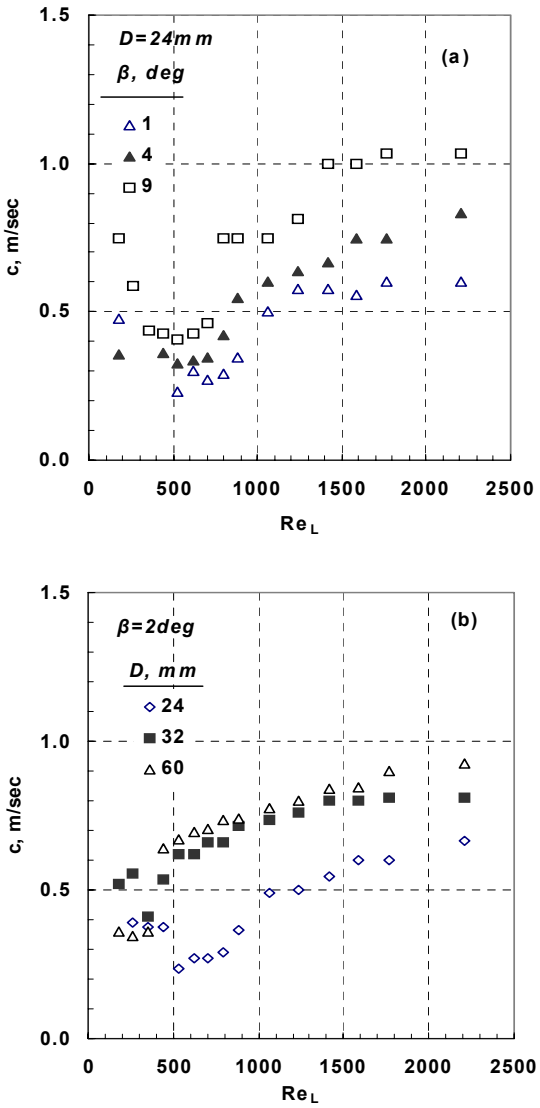

Figure 8. Dependence of wave celerity on Re_L for: (a) various inclinations; (b) various pipe diameters.

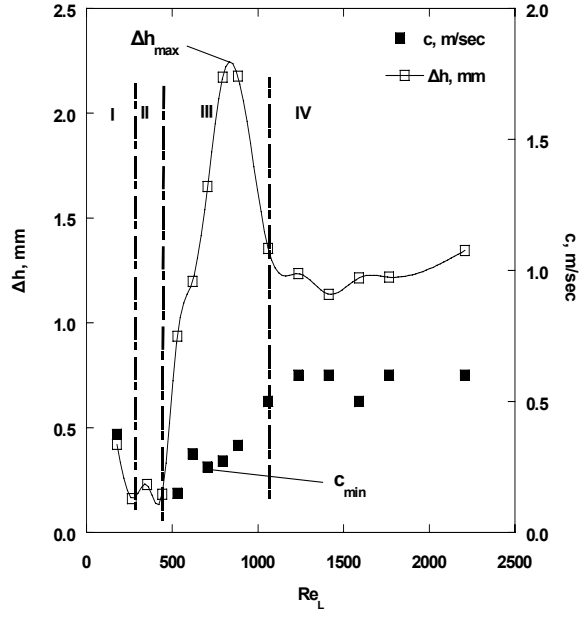

Figure 9. Wave celerity and Δh vs Reynolds number, β=1deg, D=24mm.

To take into account the type of flow prevailing in the range of our experiments, i.e. both laminar and turbulent, a modified force balance (presented in ***Appendix A***) is employed. A comparison of the calculated mean liquid layer thickness *(dashed line)* obtained from ***Eqs. A.9*** & ***A.10*** with the estimated one *(solid line)*, based on the force balance method, is presented in ***Figure 10*** (Re_{actual} is defined by Eq. A.11). As it is expected for $Re_L<Re_{LC}$ both models give practically the same results, while for $Re_L>Re_{LC}$ (where the turbulent flow consideration is employed) the model based on the force balance solution is in better agreement with the experimental data. Consequently, the latter model, which takes into account the turbulent behavior of the liquid layer, is considered more appropriate for the study of free falling liquid layers in pipes. The measured mean liquid layer thickness, h_{mean}, is in reasonable agreement with its calculated value, h_{model} (***Figure 11***).

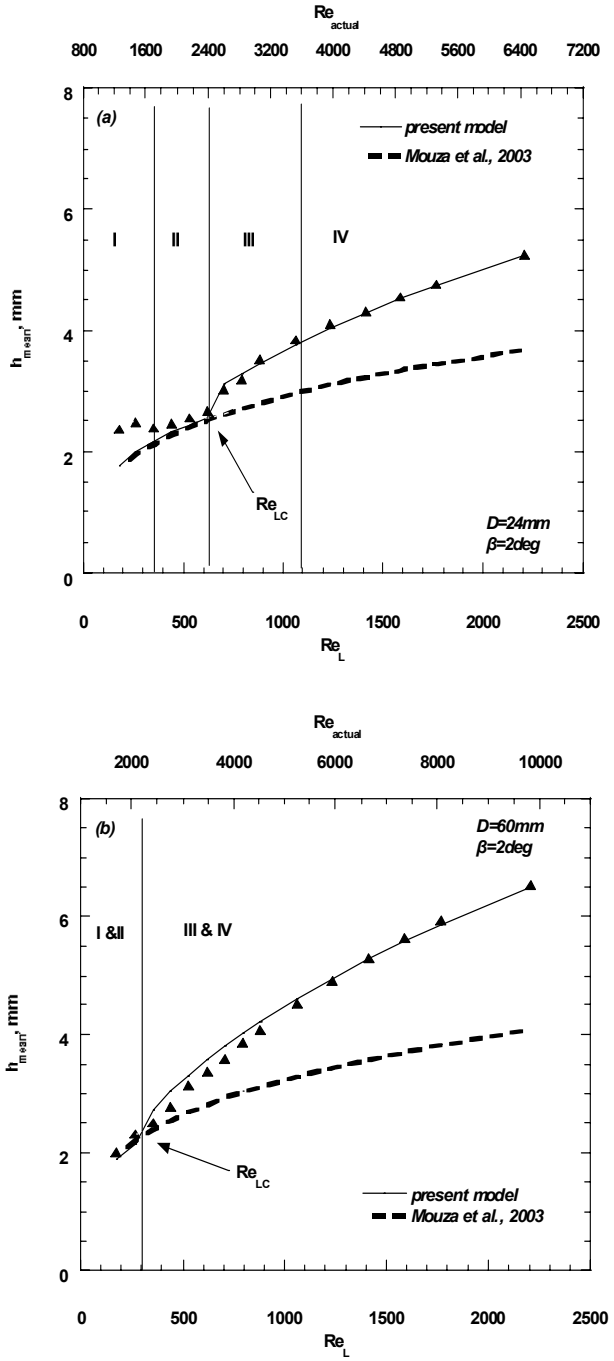

Figure 10. Comparison of h_{mean} data with theoretical predictions: (a) D=24mm; (b) D=60mm, (β=2deg).

It is evident (***Figure 10***) that as the liquid flow rate increases the mean layer thickness also increases, whereas the rate of increase changes considerably after the critical Reynolds number (Re_{LC}) is attained. A Reynolds number, Re_{TR}, which denotes the transition from laminar to turbulent flow, can be calculated (***Appendix A***):

$$\mathrm{Re}_{TR} = 7598\left(\frac{\nu_L^{\,2}}{D^3 g \sin\beta}\right)^{0.185} \qquad (3)$$

Eq. 3, which mathematically arises from the physical model, shows that laminar to turbulence transition depends on pipe diameter and inclination angle (***Figure 12***). The data points in ***Figure 12*** correspond to $Re_L=Re_{LC}$ where the first solitary wave is observed. The fact that the data are in fairly good agreement with the predictions of ***Eq. 3*** (*solid line*) could be considered as evidence that the appearance of the *first* solitary wave might be related with the transition from laminar to turbulent flow.

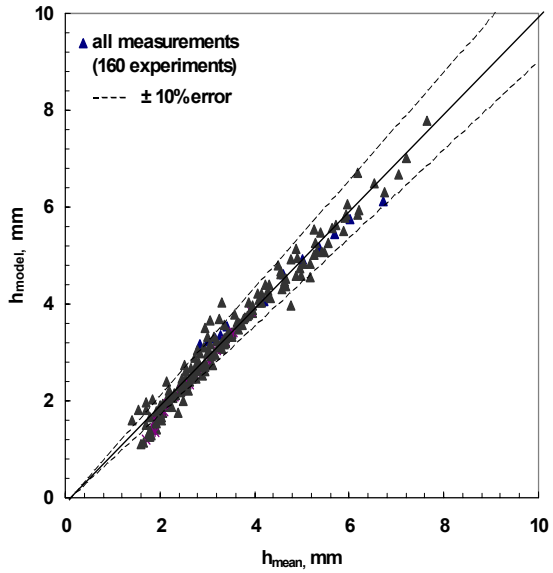

Figure 11. Comparison of h_{mean} data with model predictions.

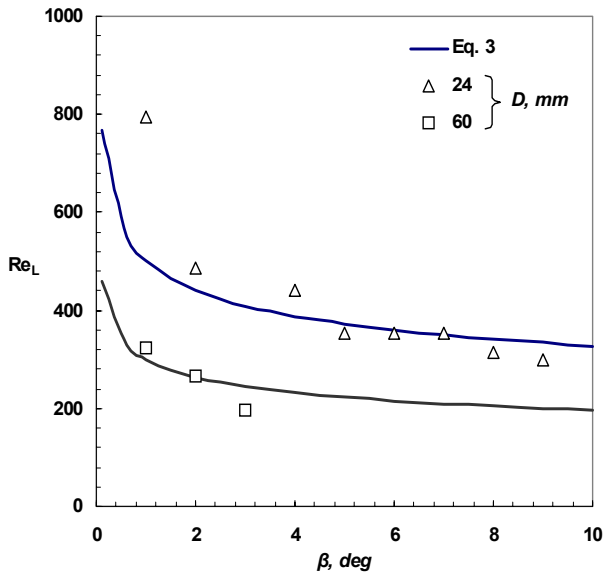

Figure 12. Effect of pipe inclination on Re_{LC} and comparison with the theoretical model (Eq. 3).

5. CONCLUDING REMARKS

New experimental data on liquid layer thickness in various diameter inclined pipes are obtained, which are expected to contribute to the understanding of the mechanisms prevailing in gas-liquid co-current flow in inclined pipes. In general, the falling layer characteristics obtained in this study provide new insights, helpful in future modelling efforts.

The visual observations reveal four distinct Re_L regions on the basis of the wave patterns observed. As the pipe inclination and diameter increase, the region boundaries are shifted to lower Re_L. A critical Reynolds number, Re_{LC} is related to the appearance of the first solitary wave which marks the transition from *Region II* to *Region III*. It is evident that, as the liquid flow rate increases, the mean layer thickness also increases, although the rate of increase changes after the critical Reynolds number (Re_{LC}) is attained. A simplified model based on a modified force balance is proposed for the prediction of the mean layer thickness based on the liquid flow rate, pipe diameter and inclination angle. The proposed model predictions are in good agreement with the experimental data and indicate that the transition from laminar to turbulent flow could be related to the passage from *Region II* to *Region III* and the appearance of solitary waves. To confirm this idea and to clarify the kind of flow prevailing inside the liquid layer, local velocity measurements using *LDA* are in progress in the Laboratory of Chemical Process and Plant Design (*A.U.Th.*). It is also believed that more theoretical work is needed, involving mainly linear/nonlinear stability theory, to help the prediction of the critical conditions for the wave evolution/development.

Acknowledgement: Mr. J. S. Lioumbas would like to thank the *CPERI*, the *State Scholarships Foundation* and the *Marie Curie Training Program* for the financial support provided.

6. NOMENCLATURE

A	cross-sectional area, m^2
C	constant in the friction factor correlation, *dimensionless*
dp/dx	average axial pressure gradient, Pa/m
D	pipe diameter, m
D_L	hydraulic diameter, m
f_m	modal wave frequency, s^{-1}
f_L	wall friction factor, *dimensionless*
g	gravitational acceleration, m/s^2
h	height of liquid layer, m
h_{mean}	mean height of liquid layer, m
h_{rms}	root mean square height of liquid layer, m
h_s	substrate thickness, m
h_w	maximum wave height, m
Δh	mean wave height above the substrate, m
n	constant in the friction factor correlation, *dimensionless*
Re_{actual}	Reynolds number based on the circular sector A_L, *dimensionless*
Re_L	superficial Reynolds number, *dimensionless*
Re_{TR}	Reynolds number (the transition from laminar to turbulent), *dimensionless*
Re_{LC}	Reynolds number (where the first solitary waves appear), *dimensionless*
Re^*	Reynolds number (where the maximum wave amplitude is observed), *dimensionless*
S	wetted perimeter, m
Q	volumetric flow rate, m^3/s
U_{LS}	superficial liquid velocity, m/s

Greek letters

β	angle of inclination, *deg*
θ	angle defined by Eq. A.2, *deg*
μ	viscosity, kg/ms
ν	kinematic viscosity, m^2/s
ρ	density, kg/m^3
τ	wall shear stress, Pa
τ_i	interfacial shear stress, Pa

7. REFERENCES

1. Karimi, G. and Kawaji, M., 1998 An experimental study of freely falling films in a vertical tube, *Chem. Eng. Science*, 53, 3501-3512.
2. Kapitza, P.L. and Kapitza, S.P., 1949 Wave flow of thin liquid layers, *Zh.Eksp. Teor. Fiz.*, **19**, 105-120.
3. Binnie, A.M., 1957 Experiments on the onset of the wave formation on a film of water flowing down a vertical plate, *J. Fluid Mech*., **2**, 551-553.
4. Jones, L.O. and Whitaker S., 1966 Experimental study of falling liqud films, *AIChE J.*, **12**, 525-529.
5. Telles, A.S. and Dukler, A.E., 1970 Statistical characteristics of thin vertical wavy liquid films, *Ind. Eng. Chem. Fund*., **9**, N 3, 412-421.
6. Brauner, H. and Maron, D.M., 1983 Modeling of wavy flow inclined thin films, *Chem. Eng. Sci*., **38**, N 5, 775-788.
7. Vlachogiannis, M. and Bontozoglou, V., 2001 Observations of solitary wave dynamics of film flows. *J. Fluid Mech.*, **435**, 191-215.
8. Wilkes, J.O. and Nedderman, P., 1962 The measurement of velocities in thin films of liquid, *Chem. Eng. Sci.*, **17**, 177-187.
9. Stainthorp, F.P. and Allen, J.M., 1965 The Development of Ripples on the Surface of Liquid Film Flowing Inside a Vertical Tube, *Trans. Inst- Chem*. Eng., **43**, T85-T91.
10. Giovine, P., Minervini, A. and Andreussi. P., 1990 Stability of liquid flow down an inclined tube, *Intern. J. Multiphase Flow,* **17**, 485-496.
11. Mouza, A.A., Paras, S.V. and Karabelas, A.J., 2002 The influence of small tube diameter on falling film and flooding phenomena. *Intern. J. Multiphase Flow* **28**, 8, 1311-1331.
12. Paras, S.V. and Karabelas, A.J., 1991 Properties of the liquid layer in horizontal annular flow. *Intern. J. Multiphase Flow* **17**, 39, 454.
13. Lilleby, K., 2001 User's Manual for Multiphase Flow Loop, NTNU.
14. Patnaik, V. and Blanco, H.P., 1996 Roll waves in falling films: an approximate treatment of the velocity field, *Int. J. Heat and Fluid Flow* 63-70.
15. Park, C.D. and Nosoko, T., 2003 Three-Dimensional wave dynamics on a falling film and associated mass transfer, *AIChE J*., **49**, 11, 2715-2727.
16. Mouza, A.A., Paras, S.V. and Karabelas, A.J., 2003 Incipient flooding in inclined tubes of small diameter. *Intern. J. Multiphase Flow* **29**, 8, 1395-1412.
17. Schlichting, H., 1960 Boundary layer theory; 4th Ed. (McGraw-Hill, New York).
18. Taitel, Y. and Dukler, A.E., 1976 A model for predicting flow regime transitions in horizontal and near horizontal gas-liquid flow, *AIChE J*., **22**, 7, 47-55.

APPENDIX A

Free flow of a thin liquid layer in inclined tube

The flow geometry is defined in ***Figure A1.***

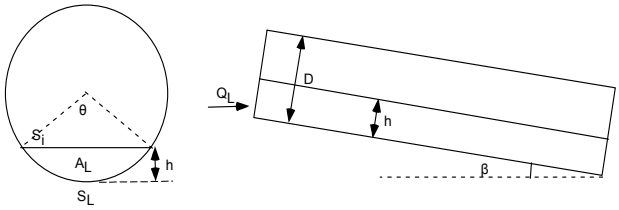

Figure A1. System coordinates and parameters

The force balance for the liquid phase is:

$$-A_L \frac{dP}{dx} - \tau_L S_L - \tau_i S_i + \rho_L A_L g \sin\beta = 0 \qquad \text{(A.1)}$$

The following assumptions are made to simplify ***Eq. A.1***:

- Flat free surface, with a free flowing layer thickness, given by

$$h = \frac{D}{2}(1-\cos\theta) \qquad \text{(A.2)}$$

- $\tau_i = 0$ and
- $dP/dx = 0$

The shear stress and the liquid friction factor are evaluated in the conventional manner [17, 18]:

$$\tau_L = f_L \frac{\rho_L U_L^2}{2}\ , \qquad \text{(A.3)}$$

$$f_L = C_L\left(\frac{A_L \nu_L}{D_L Q_L}\right)^n \qquad \text{(A.4)}$$

where $D_L = 4A_L/S_L$ is the hydraulic diameter as suggested by Taitel & Dukler [18]. By substituting ***Eqs. A.2, A.3*** and ***A.4*** in ***Eq. A.1*** we obtain:

$$\frac{S_L^{\,n+1}}{A_L^{\,3}} = \frac{2^{2n+1} g \sin\beta}{C_L Q^{2-n} \nu_L^{\,n}}\theta \qquad \text{(A.5)}$$

where $C_L = 0.046$, $n = 0.2$ for *turbulent* flow and $C_L = 16$, $n = 1.0$ for *laminar* flow. ***Eq. A.5*** is a function of $\boldsymbol{\theta}$ and by substituting S_L and A_L (from the pipe geometry):

$$S_L = \theta\frac{D}{2} \text{ and } A_L = \frac{D^2}{2}(\theta - \sin\theta) \qquad \text{(A.6)}$$

Eq. A.5 becomes:

$$\frac{\theta^{n+1}}{(\theta-\sin\theta)^3} = \frac{2^{3n-7} D^{5-n} g \sin\beta}{C_L Q^{2-n} \nu_L^{\,n}} \qquad \text{(A.7)}$$

and it is solved analytically by applying Taylor-series transformation:

$$\frac{\theta^{n+1}}{(\theta-\sin\theta)^3} = \theta^{n+1}\left(\frac{216}{\theta^9} + \frac{162}{5\,\theta^7} + \ldots\right) \approx$$

$$\approx \theta^{n+1}\left(\frac{216 + \frac{162}{5}}{\theta^9}\right) \qquad \text{(A.8)}$$

Eq. A.8 is solved for laminar and turbulent flow (using the appropriate coefficients for each case) and gives:

$$\theta = 5.155\left(\frac{Q_L \nu_L}{D^4 g \sin\beta}\right)^{0.142}, \textit{ laminar flow} \qquad \text{(A.9)}$$

$$\theta = 2.480\left(\frac{Q_L^{\,1.8} \nu_L^{\,0.2}}{D^{4.8} g \sin\beta}\right)^{0.128}, \textit{turbulent flow} \qquad \text{(A.10)}$$

Thus, for given Q_L, D, β, the layer thickness h can be calculated using ***Eqs. A.9***, ***A.10*** and ***A.2*** provided that the laminar to turbulent transition criterion (Re=2200) [17, 18] is taken into account. It must be noted that Re_{actual} is based on the actual circular sector A_L, (***Figure A.1***) and defined as:

$$\mathrm{Re}_{actual} = \frac{D_L U_L}{\nu_L} = \frac{4A_L}{S_L}\frac{1}{\nu_L}\frac{Q_L}{A_L} = \\ = \frac{4Q_L}{S_L \nu_L} = \frac{8Q_L}{\theta D \nu_L} = \frac{2\pi}{\theta}\mathrm{Re}_L \qquad \text{(A.11)}$$

By setting Re_{actual}=2200 and using ***Eqs. A.11*** and ***A.9***, the transition Reynolds number, Re_{TR}, based on the superficial liquid velocity can be expressed as a function of D and β.

$$\mathrm{Re}_{TR} = 7598\left(\frac{\nu_L^{\,2}}{D^3 g \sin\beta}\right)^{0.185} \qquad \text{(A.12)}$$

It is obvious that at the transition point ***Eqs. A.9*** and ***A.10*** give the same value for the layer thickness.